Available online at www.sciencedirect.com
ScienceDirect
Trans. Nonferrous Met. Soc. China 29(2019) 2463−2471
Transactions of Nonferrous Metals Society of China
www.tnmsc.cn

Effects of zinc content on strength and wear performance of Al−12Si−3Cu based alloy

Yasin ALEMDAG[1], Murat BEDER[2]

1. Department of Mechanical Engineering, Karadeniz Technical University, Trabzon 61100, Turkey;
2. Department of Mechanical Engineering, Gumushane University, Gumushane 29100, Turkey

Received 6 March 2019; accepted 21 August 2019

Abstract: The effects of Zn content on strength and wear performance of Al−12Si−3Cu alloy synthesized by gravity casting were systematically investigated. The microstructure and mechanical properties of the alloys were evaluated using OM, XRD, SEM as well as hardness, tension, compression and Charpy impact tests. Their dry sliding wear tests were carried out with a ball-on-disk tester. Microscopic examinations revealed that the microstructure of the base alloy consisted of the α(Al) dendrites, needle-type and coarse Si particles, and $CuAl_2$ (θ) phase. The addition of Zn to this alloy resulted in the formation of α-solid solution phase and the increase of coarse Si particles. The hardness, yield, tensile and compressive strengths, elongation to fracture and impact toughness of the Al−12Si−3Cu−Zn alloys increased with increasing Zn content, but tendency in the tensile and compressive strengths and ductility reversed after adding 1.5%−2% Zn. In addition, the friction coefficient and volume loss of the Al−12Si−3Cu−Zn alloys decreased with increasing Zn content. The study showed that the addition of Zn to Al−12Si−3Cu alloy can improve its potential applications as tribological material.

Key words: Al−Si−Cu alloy; Zn content; microstructure; mechanical properties; wear performance

1 Introduction

The binary eutectic Al−12Si casting alloy has very excellent properties such as high fluidity and low shrinkage in casting, low thermal expansion coefficient, high specific strength, and appropriate corrosion and wear resistance [1,2]. The strength and wear properties of this alloy are improved by using alloying elements such as copper and magnesium due to their solid solution strengthening and precipitation hardening effects [3−5]. Through extensive experimental studies a series of Al−12Si−Cu and Al−12Si−Mg alloys are developed for internal combustion engines in automotive and aerospace applications [6,7]. The engine parts including cylinder blocks, heads and liners, pistons, and water cooled manifolds are produced from these alloys. In addition, the Al−12Si−Cu and Al−12Si−Mg alloys have also been used for the sliding bearing materials replacing cast iron, bronze and brass [1,2]. The Al−12Si−Cu alloys exhibit higher strength and better wear resistance than Al−12Si−Mg alloys at both ambient and elevated temperatures [8−10]. The addition of copper in the range of 1%−4% to the eutectic alloy gives rise to a satisfactory improvement of the strength and wear resistance in ordinary service conditions [1,2]. Therefore, Al−12Si−(1−4)Cu alloys are taken as the base material in wide range engineering applications [11−13].

In most of engineering applications, the Al−12Si−Cu alloys are used by alloying with a small amount of Mg, Mn, Ni and Zn [7,12−15]. The magnesium addition increases the strength and wear properties of Al−12Si−Cu based alloys due to the formation of hard precipitate of Mg_2Si phase in matrix [11,13]. Mn, on the other hand, reduces the amount of brittle plate-like Al_5FeSi phase in the interdendritic region of Al−12Si−Cu alloys containing Fe and increases their ductility [12]. Moreover, Mn and Ni enhance their strength and hardness at elevated temperatures [12,13]. The addition of small amount of Zn improves the hardness of Al−12Si−Cu alloys after heat treatment [1]. However, Zn has higher solubility in aluminum matrix alloy compared with other alloying elements such as Mn, Mg, Ni and Fe since its atomic radius is almost equal to that of Al [16]. In addition, Zn and its oxide have good lubrication characteristics and serve as solid lubricant under dry

Corresponding author: Yasin ALEMDAG; Tel: +90-462-3774134; E-mail: yalemdag@ktu.edu.tr
DOI: 10.1016/S1003-6326(19)65154-X

sliding conditions [17]. In this context, it can be thought that the increase in the amount of Zn can enhance the strength and wear performance of the Al−12Si−Cu alloys. Therefore, the main purpose of the present study is to investigate the effect of Zn content in a specific range on the microstructure, strength, friction and wear properties of the Al−12Si−3Cu based alloy and to determine its optimum chemical composition for tribological applications.

2 Experimental

2.1 Production of alloys and microstructure

The Al−12Si−3Cu−Zn alloys were prepared from high-purity Al (99.7%), Zn (99.9%), Al−20Si and Al−50Cu intermetallics. These materials were melted at 700 °C in graphite crucible heated with electricity, stirred and cast at 690 °C into the conical shape mould. The mould was fabricated from mild steel with dimensions of *d*57 mm × *d*70 mm × 180 mm. After the solidification was completed, the ingots were taken out from the mould and their chemical compositions were analyzed by using spectral analysis. The densities of the alloys were calculated in accordance with mass-to-volume ratio.

The microstructures of the alloys were examined with optical microscopy (OM) and X-ray diffractometry (XRD). For OM studies, metallographic samples were mounted in a hot resin, ground with emery paper, polished with diamond suspension and etched with nitric acid (6% HNO_3 + 94% alcohol) solution. The XRD analysis was conducted on flat samples in scanning range from 20° to 80° and scanning speed of 3 (°)/min using Cu K_α radiation.

2.2 Mechanical tests

The Brinell hardness of the produced alloys was measured using a ball indenter with a diameter of 2.5 mm at a load of 625 N. Vickers microhardness of α-matrix was determined under a load of 490.6l mN. The tensile and compressive properties of the alloys were studied on the dog-bone and cylinder shape samples, respectively. The dog-bone samples were fabricated by wire-EDM having a thickness of 2.5 mm, a width of 5.6 mm and a gage length of 20 mm, while the cylindrical samples with 10 mm in diameter and 10 mm in length were prepared by machining from the alloys. These tests were performed at a strain rate of 5×10^{-4} s^{-1} and room temperature. The strength value in 50% deformation of the samples was taken to be a compressive strength in all compression tests. The impact toughness test of the alloys was carried out using the Charpy impact tester. This test studied on the rectangular samples with dimensions of 10 mm × 10 mm × 50 mm. The tensile, compressive and impact tests were repeated at least three times, while five readings were taken for hardness tests to check the accuracy of the results. After the tensile test, the perpendicular sections of tensile fracture surface of the samples were analyzed by SEM with energy dispersive spectrometry (EDS), while OM was used to examine their longitudinal cross sections.

2.3 Friction and wear tests

The friction and wear properties of the alloys were studied in dry sliding conditions by using a ball-on-disc type tribotest machine governed by a software. This machine was constructed according to ASTM G99. The schematic appearance of its main components and test region of tribotester are shown in Fig. 1. The friction and wear samples with dimensions of *d*24 mm × 10 mm were produced from the alloys using wire-EDM. Before the test, these samples were polished in automatic polishing machine, cleaned ultrasonically in acetone and weighed using a precision balance having a sensitivity of 0.01 mg. After these processes, the samples were put on the rotating disc and abraded with an ASTM 52100 steel ball having a diameter of 6 mm. The friction and wear tests

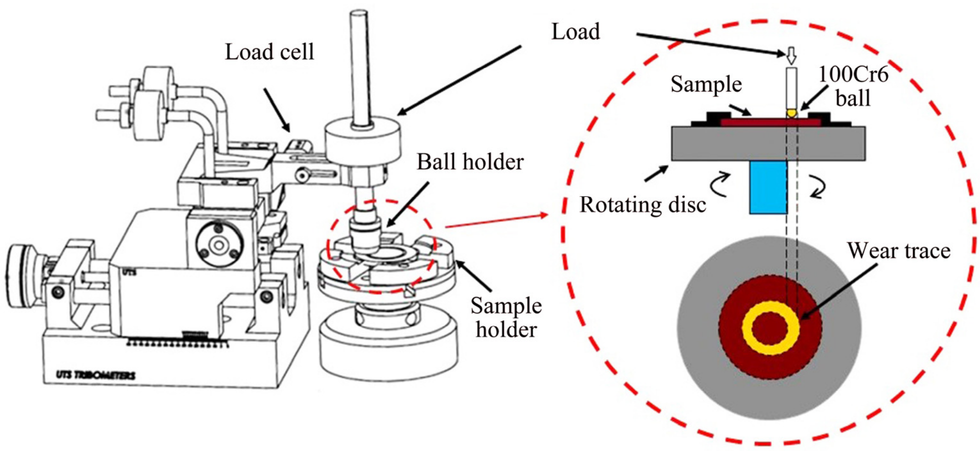

Fig. 1 Schematic appearance of main components and test region of tribotester (UTS tribometers, www.uts-design.com)

were carried out under a load of 5 N at a sliding speed of 0.16 m/s and a sliding distance of 1000 m. After run was completed, the samples were removed, cleaned and weighed again. The difference in mass of samples before and after wear testing was taken as the mass loss due to wear, and this value was converted into volume loss by using the density of the alloys. Each test was repeated three times. The worn surfaces of the samples, wear debris generated during the wear and ball surfaces were examined with SEM−EDS to determine the wear mechanism of the alloys.

3 Results

3.1 Microstructures

The chemical compositions and densities of the alloys are given in Table 1. As seen in Table 1, the chemical compositions of the alloys are almost the same as their nominal compositions. Table 1 also shows that densities of the alloys increase with increasing Zn content. The microstructures and XRD patterns of the alloys are presented in Fig. 2 and Fig. 3, respectively.

Table 1 Chemical compositions and densities for all alloys

Alloy	Content/wt.%				Density/($g\cdot cm^{-3}$)
	Al	Si	Zn	Cu	
Al−12Si−3Cu	83.97	12.9	0.03	3.10	2.680
Al−12Si−3Cu−0.5Zn	83.60	12.7	0.60	3.10	2.720
Al−12Si−3Cu−1Zn	83.30	12.7	0.90	3.10	2.730
Al−12Si−3Cu−1.5Zn	82.43	12.9	1.70	2.97	2.735
Al−12Si−3Cu−2Zn	82.10	12.8	2.10	3.00	2.746
Al−12Si−3Cu−2.5Zn	81.60	12.9	2.50	3.00	2.753

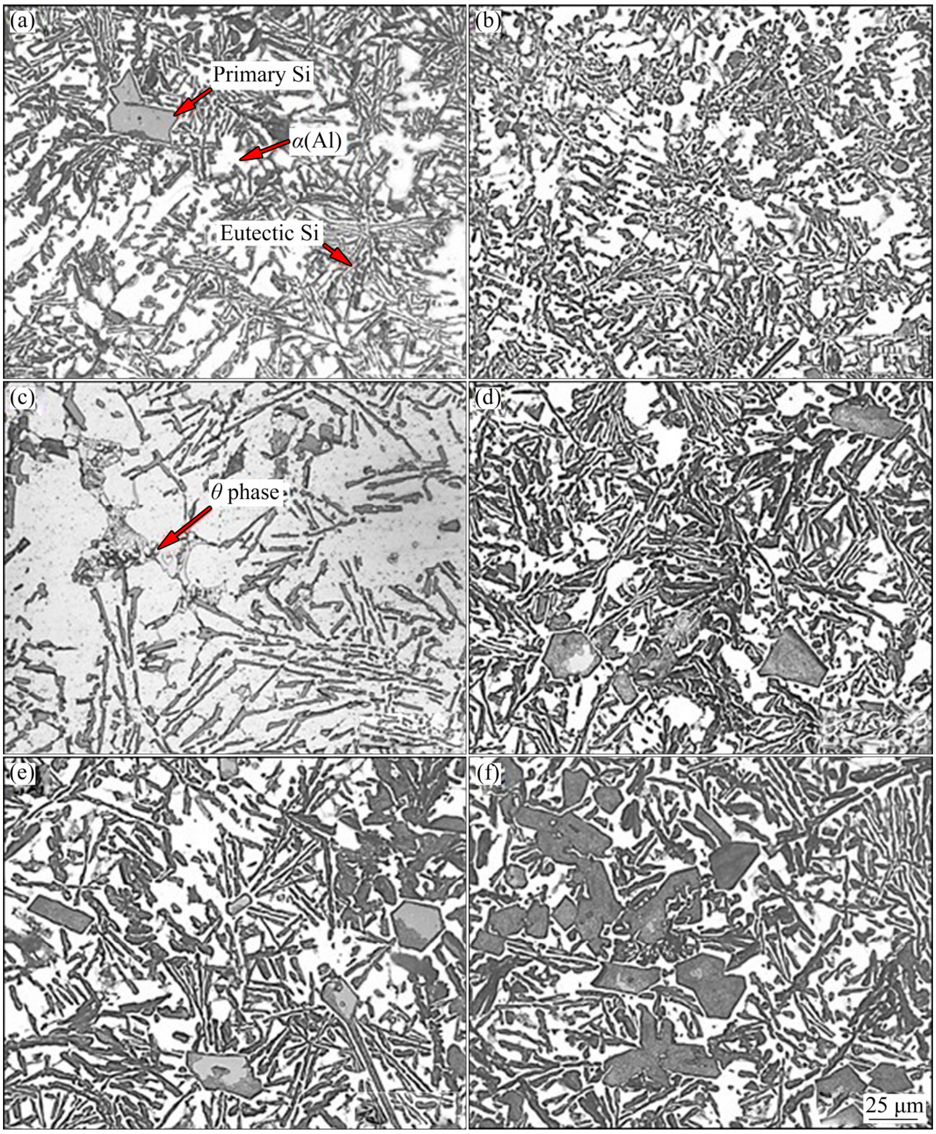

Fig. 2 Optical micrographs of different alloys: (a) Al−12Si−3Cu; (b) Al−12Si−3Cu−0.5Zn; (c) Al−12Si−3Cu−1Zn; (d) Al−12Si−3Cu−1.5Zn; (e) Al−12Si−3Cu−2Zn; (f) Al−12Si−3Cu−2.5Zn

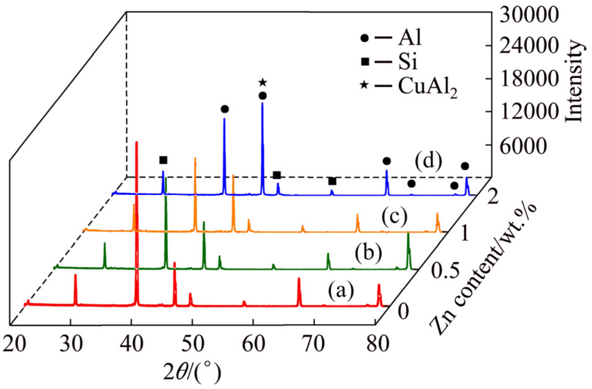

Fig. 3 XRD patterns of different alloys: (a) Al−12Si−3Cu; (b) Al−12Si−3Cu−0.5Zn; (c) Al−12Si−3Cu−1Zn; (d) Al−12Si−3Cu−2Zn

The microstructure of base alloy is composed of α(Al) matrix, copper-rich $CuAl_2$ (θ) phase, needle-like and a few coarse Si particles, as shown in Fig. 2(a). The alloys containing Zn have similar microstructures with the base alloys, but the addition of Zn causes a significant increase in the number of coarse Si particles and their segregation in the α(Al) matrix of the alloys, as shown in Figs. 2(b−f). The presence of observed phases in the microstructure of the alloys is proved by the XRD results which represent their characteristic peaks.

3.2 Mechanical properties

The tensile, yield, compressive, hardness and impact tests results are given in Figs. 4−6 according to Zn content, respectively. Figure 4 shows that the yield, tensile and compressive strengths of alloys increase up to Zn content of 2%, then they start decreasing after this content. The hardness properties exhibit a sharp increase up to 1% Zn, remain almost constant at 1%−2% Zn before the final increase after 2% Zn, as shown in Fig. 5. Figure 6 shows that Zn contents up to 1.5% and 2% improve the impact toughness and elongation to fracture of the alloys, respectively. These properties exhibit decrease beyond these levels. The appearance of the

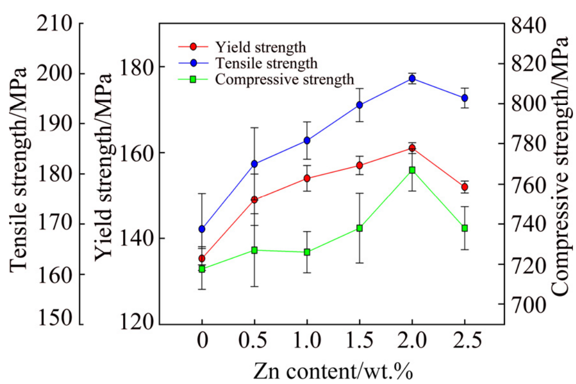

Fig. 4 Tensile, yield and compressive strength values of alloys

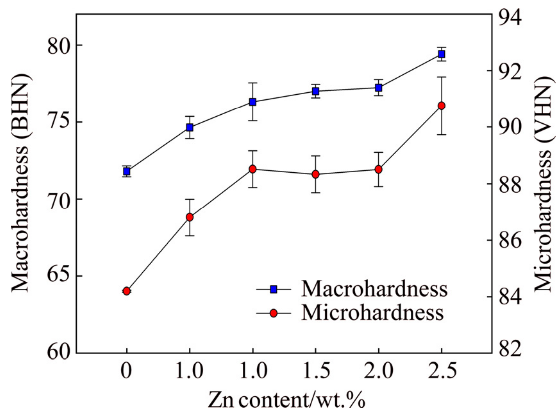

Fig. 5 Macrohardness and microhardness of alloys

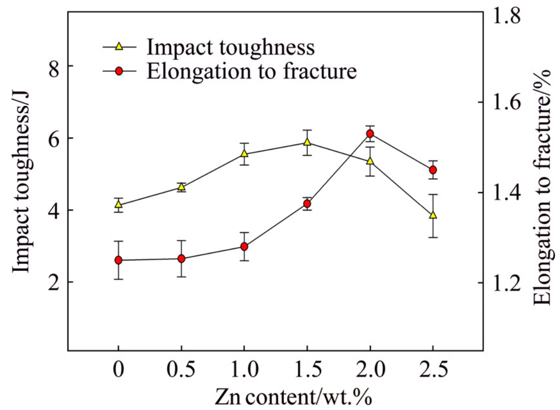

Fig. 6 Impact toughness and elongation of alloys

tensile fracture surface of the selected alloys is depicted in Fig. 7 to explain their fracture type. Figures 7(a, c, e) show that tensile fracture surfaces of the alloys are composed of the facets (flat areas) and hills, but the facets appear to be characteristic feature of their fracture surfaces. Figures 7(b, d, f) show that the facets are formed by the rupture of the Si particles and/or their torn-off from α(Al) phase, while the rupture of soft α(Al) phase results in the formation of hills on their surface. It is also observed that the size of facets increases with the increase of the Zn content.

3.3 Friction and wear performance

The change in the friction coefficient of the alloys with sliding distance is shown in Fig. 8, which indicates that the friction coefficients of the alloys decrease after exhibiting an initial increase with increasing sliding distance and attain almost steady-state values. However, their friction coefficients in this period show a trend including repeated increment and decrement. The average friction coefficient of the alloys at steady-state and their volume loss with Zn content during the sliding process are plotted in Fig. 9. This figure shows that the friction coefficients and volume loss of the alloys decrease continuously with increasing the Zn content.

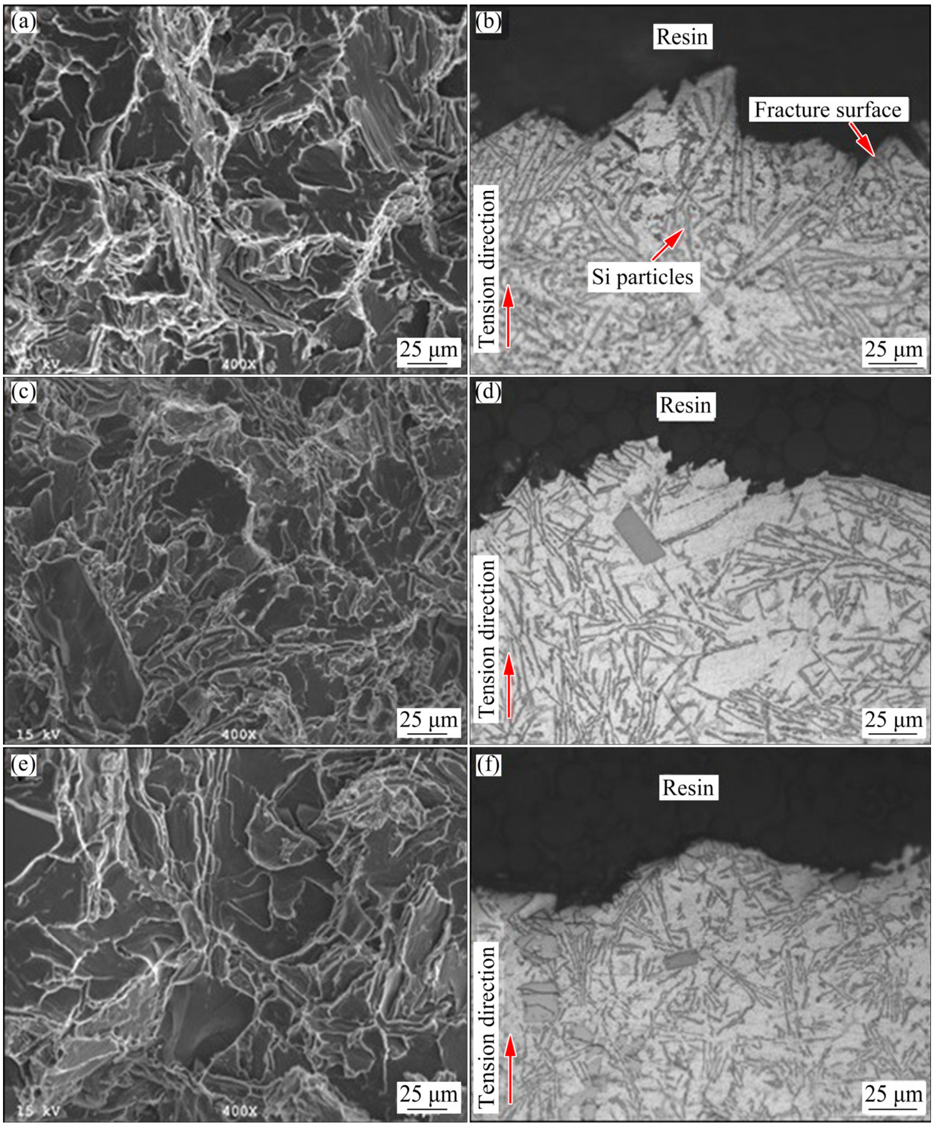

Fig. 7 Appearance of fracture surface: (a, b) Al−12Si−3Cu; (c, d) Al−12Si−3Cu−1Zn; (e, f) Al−12Si−3Cu−2Zn

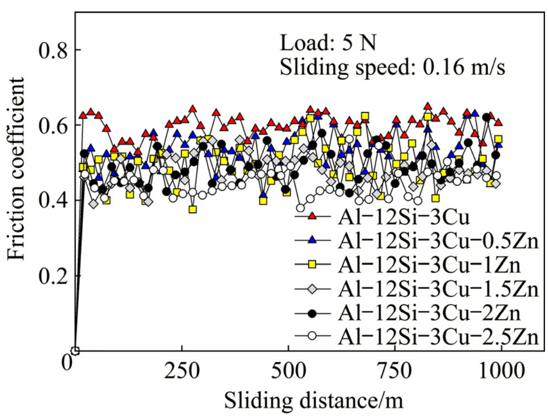

Fig. 8 Change in friction coefficient with sliding distance

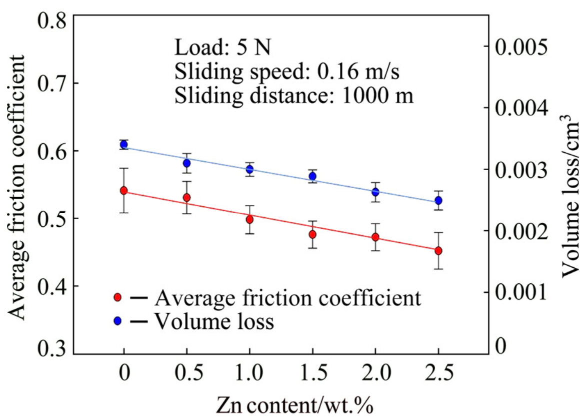

Fig. 9 Average friction coefficient and volume loss of alloys with Zn content

Due to similarity in the worn surfaces of the alloys after the wear test, only SEM images of the worn surfaces of Al−12Si−3Cu and Al−12Si−3Cu−2Zn alloys are shown in Fig. 10 as representative. In addition, the results of the EDS analysis on worn surfaces are documented on these images. Figure 10 shows that the smearing, delamination and oxidation are the characteristic features of the worn surfaces of the alloys. However, smearing is found to be more effective feature for the alloys. It is also found that the smearing areas contain high amount of oxygen in addition to the Al, Si, Cu and Zn.

The SEM−EDS examinations on the ball surfaces and wear fragments are given in Figs. 11 and 12 for the selected alloys, respectively. Figure 11 shows that the ball surfaces are coated by the material having almost the same composition with that of smearing areas on the worn surfaces of the alloys. Fig. 12 shows that the wear particles consist of fine and large size particles containing small amount of Fe and Cr besides Al, Si, Cu and Zn. On the other hand, it is observed that the amount of the large size particles decreases with increasing Zn content.

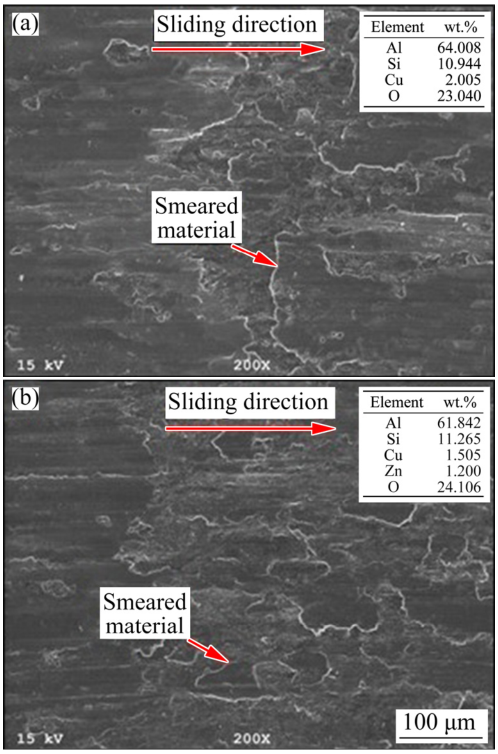

Fig. 10 SEM−EDS analysis results of worn surface: (a) Al−12Si−3Cu; (b) Al−12Si−3Cu−2Zn

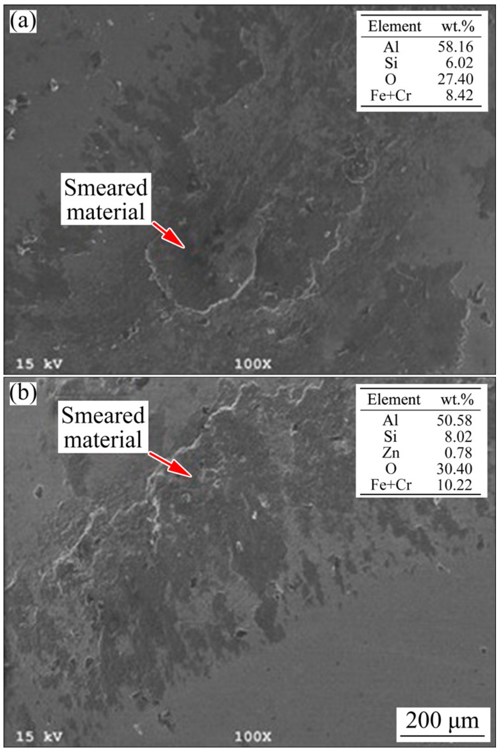

Fig. 11 SEM−EDS analysis results of ball surfaces: (a) Al−12Si−3Cu; (b) Al−12Si−3Cu−2Zn

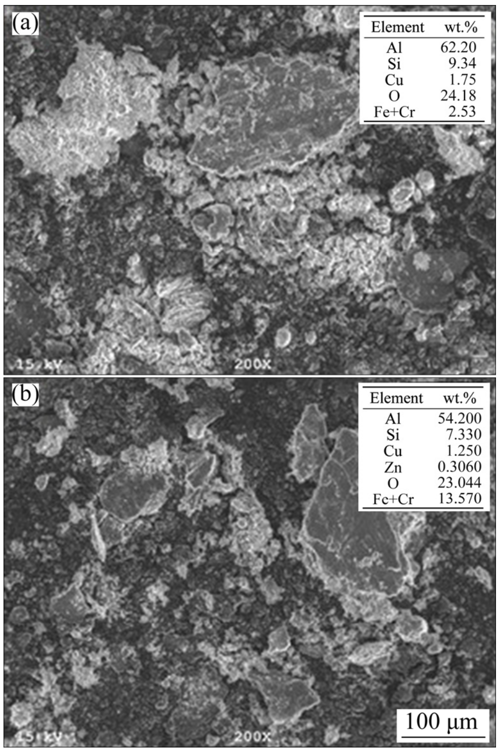

Fig. 12 SEM−EDS analysis results of wear fragments: (a) Al−12Si−3Cu; (b) Al−12Si−3Cu−2Zn

4 Discussion

The microstructure of the base alloy consisted of α(Al) dendrites, eutectic mixture of Al−Si mixture, a few coarse Si particles and θ-phase. The morphologies of the alloys containing Zn were observed to be quite similar to that of base alloy. Moreover, XRD results showed that there were no peaks representing Zn compounds, which meant that Zn was completely dissolved α(Al) phase due to its higher solubility in Al [17]. However, the number of coarse Si particles increased with increasing Zn content and these particles caused a segregation by grouping in the matrix. This might be related to the shifting of the eutectic point towards to the hypoeutectic side and lowering in eutectic temperature due to Zn content as mentioned in previous studies [18−20].

The addition of Zn to base alloy improved its tensile and compressive strengths as well as its macrohardness and microhardness of α(Al) matrix, as seen in Figs. 4 and 5. The highest tensile and compressive strengths were obtained with Al−12Si−3Cu−2Zn alloy, while Al−12Si−3Cu−2.5Zn exhibited the highest macrohardness and microhardness among the alloys. The improvement in these properties can be attributed to the solid solution strengthening effect of Zn [16,21]. However, the addition of Zn to the alloys caused the segregation of coarse Si particles. This can reduce the tensile and compressive strengths of the alloys after 2% Zn content by suppressing its strengthening effect [18,22].

Zn addition up to 1.5% and 2% resulted in a slight increase in the impact toughness and elongation to failure of the alloys, while they started decreasing after these levels, respectively, as shown Fig. 6. The slight increase in these values may be related to the increase in the number of the coarse Si particles. As the number of coarse Si particles increases, it can be expected that the volume fraction of the needle-like Si particles can decrease [23−26]. Since the needle-like Si particles have sharp tips, they are more prone to form a crack in the matrix than the coarse ones which restrict plastic deformation of the alloys [24−26]. Therefore, the decrease in volume fraction of needle particles can increase plastic deformation capacity of the alloys and brings about slight improvement in their toughness and ductility. However, the segregation of coarse Si particles can result in the drop in these values by restricting the plastic deformation capacity of the alloys with 1.5%−2% Zn.

The tensile fracture surfaces of the alloys were composed of the facets and hills, but the facets appeared to be the main feature of their fracture surfaces, as shown in Figs. 7(a, c, e). These observations can be attributed to the cracking tendency effect of the Si particles. It is well known that the Si particles behave as stress riser points and crack initiation sites due to poor deformation capacity of Si crystal and its low interface bonding [24−26]. Microscopic examination on fracture surfaces showed that the cracks initiated by the rupture of Si particles and/or their torn-off from soft α(Al) phase, as shown in Figs. 7(b, d, f). These cracks propagated in the interdendritic regions and caused to the cleavage type intergranular fracture of the alloys. This type of fracture resulted in the formation of a lot of flat facets and hills on the tensile fracture surface of the alloys. The increase in size of the facets with respect to Zn content of the alloys can be related to the segregation of coarse Si particles in the α(Al) matrix [25].

The friction coefficient of the alloys increased at starting of test and then reached the stable-state with increasing sliding distance, as shown in Fig. 8. This can be a result of the adhesion between rubbing surfaces [27,28]. At the start of run, the rubbing surface can adhere together due to high contact pressure. This adhesion can cause an increase in the friction force necessary for sliding. The contact pressure can approach the constant value with the increase of the contact area at subsequent sliding. When the pressure becomes constant, the friction coefficient can attain the stable-state. At this state, it exhibits a trend consisted of consecutive increment and decrement in short intervals. This can be related to the material transfer caused by adhesion at this state.

It was determined that the average friction coefficient and the volume loss of the alloys decreased with increasing Zn content, as seen in Fig. 9. These results can be explained by three different reasons, mainly strengthening effect of Zn on the alloys, the lubricant characteristic of zinc oxide, and the increase of volume fraction of the coarse Si particles [17,18,21,29,30]. Strengthening effect of Zn resulted in an increase in strength and hardness of the alloys while its oxide can behave as solid lubricant between rubbing surfaces due to its HCP structure and good smearing characteristic [17]. Moreover, volume fraction increase of the coarse Si particles supports the load between contact surfaces due to their higher hardness [29,30]. These integral effects yielded the decrease in the friction coefficient and the volume loss of the Al−12Si−3Cu−Zn alloys.

The smearing, delamination and oxidation were observed to form on the worn surfaces of the tested alloys, as seen in Fig. 10. However, smearing was found to the most effective among them. As explained by previous works [30−32], smearing took place by transfer and back transfer of wear material between ball and sample surfaces. During the subsequent sliding, this layer became thicker and its brittleness increased due to work hardening and oxidation [30−34]. When the smeared layer reached a critical thickness, micro cracks formed on the surface and/or sub-surface of the layer. Propagation of cracks resulted in delamination of this layer and produced large size wear particles [33,34]. The EDS analysis proved that the smearing layer on counter surfaces and wear particles had almost the same chemical composition, as seen in Figs. 11 and 12. This suggested that smearing was produced by material transfer between rubbing surfaces, while delamination took place due to breaking up this layer during the sliding. The decrease observed in the amount of large size wear particles with increasing Zn content can be related to good smearing characteristic of ZnO [17].

5 Conclusions

(1) The microstructure of Al−12Si−3Cu consisted of α(Al) dendrites, θ-phase, and needle-like and coarse

silicon particles. The addition of Zn to this alloy caused the formation of α-solid solution and increasing number of coarse Si particles.

(2) The hardness of the Al−12Si−3Cu−Zn alloys increased continuously with increasing Zn content. However, their yield, tensile and compressive strengths exhibited increase up to 2% Zn, above this level they decreased as the Zn content increased.

(3) The Zn content up to 1.5% and 2% resulted in an increase in impact toughness and elongation to fracture of the Al−12Si−3Cu−Zn alloys, respectively. When the Zn content of the alloys exceeded these levels, they decreased.

(4) The Al−12Si−Cu−Zn alloys showed that the cleavage-type intergranular fracture depending upon the facets and hills was observed on their tensile fracture surfaces.

(5) The friction coefficient and volume loss of the Al−12Si−3Cu−Zn alloys decreased with increasing Zn content.

(6) The smearing, delamination and oxidation were found to be characteristic morphology of the worn surfaces of the tested alloys, and the smearing was the most effective.

Acknowledgments

This study was performed in Karadeniz Technical University. The authors would like to thank all staffs in the Material Science Laboratory of Mechanical Engineering Department for their supports.

References

[1] YE H Z. An overview of the development of Al−Si alloy based material for engine applications [J]. J Mater Eng Perform, 2003, 12: 288−297.

[2] DWIVEDI D K. Adhesive wear behaviour of cast aluminium−silicon alloys: Overview [J]. Mater Design, 2010, 31: 2517−2531.

[3] ZHENG Y, XIAO W L, GE S J, ZHAO W T, HANADA S, MA C L. Effects of Cu content and Cu/Mg ratio the microstructure and mechanical properties of Al−Si−Cu−Mg alloys [J]. J Alloy Compounds, 2015, 649: 291−296.

[4] MA Z, SAMUEL E, MOHAMED A M A, SAMUEL A M, SAMUEL F H, DOTY H W. Parameters controlling the microstructure of Al−11Si−2Cu−Mg alloys [J]. Mater Design, 2010, 31: 902−912.

[5] SUN Y, AHLATCI H. Mechanical and wear behaviors of Al−12Si−*X*Mg composites reinforced with in situ Mg_2Si particles [J]. Mater Design, 2011, 32: 2983−2987.

[6] BASAVAKUMAR K G, MUKUNDA P G, CHAKRABORTY M. Dry sliding wear behaviour of Al−12Si and Al−12Si−3Cu cast alloys [J]. Mater Design, 2009, 30: 1258−1267.

[7] ANASYIDA A S, DAUD A R, GHAZALI M J. Dry sliding wear behaviour of Al−12Si−4Mg alloy with cerium addition [J]. Mater Design, 2010, 31: 365−374.

[8] ZEREN M. Effect of copper and silicon content on mechanical properties in Al−Cu−Si−Mg alloys [J]. Journal of Materials Processing Technology, 2005, 169: 292−298.

[9] BIROL Y. Semisolid processing of near-eutectic and hypereutectic Al−Si−Cu alloys [J]. J Mater Sci, 2008, 43: 3577−3581.

[10] ZEREN M, GUMUS S, KARAKULAK E. Influence of Cu addition on microstructure and hardness of near-eutectic Al−Si−*x*Cu alloys [J]. Transactions of Nonferrous Metals Society of China, 2011, 21: 1698−1702.

[11] MA Z, SAMUEL A M, SAMUEL F H, DOTY H W, VALTIERRA S. A study of tensile properties in Al−Si−Cu and Al−Si−Mg alloys: Effect of beta-iron intermetallics and porosity [J]. Mat Sci Eng A, 2008, 490: 36−51.

[12] LIAO H, TANG Y, SUO X, LI G, HU Y, DIXIT U S, PETROV P. Dispersoid particles precipitated during the solutionizing course of Al−12wt.%Si−4wt.%Cu−1.2wt.%Mn alloy and their influence on high temperature strength [J]. Mat Sci Eng A, 2017, 699: 201−209.

[13] ZUO L, YE B, FENG J, KONG X, JIANG H, DING W. Microstructure, tensile properties and creep behavior of Al−12Si−3.5Cu−2Ni−0.8Mg alloy produced by different casting technologies [J]. J Mater Sci Technol, 2018, 34: 1222−1228.

[14] FARAHANY S, OURDJINI A, BAKHSHESHI-RAD H R. Microstructure, mechanical properties and corrosion behavior of Al−Si−Cu−Zn−X (X=Bi, Sb, Sr) die cast alloy [J]. Transactions of Nonferrous Metals Society of China, 2016, 26: 28−38.

[15] NEMRI Y, CHIKER N, GUEDDOUAR B, BENAMAR M E A, SAHRAOUI T, HADJI M. Effect of Mg and Zn contents on the microstructures and mechanical properties of Al−Si−Cu−Mg alloys [J]. Int J Metal Cast, 2018, 12: 20−27.

[16] DOUGLASS D L. Spinodal decomposition in Al/Zn alloys: X-ray diffraction studies [J]. J Mater Sci, 1969, 4: 130−137.

[17] PURCEK G, SAVASKAN T, KUCUKOMEROGLU T, MURPHY S. Dry sliding friction and wear properties of zinc-based alloys [J]. Wear, 2002, 252: 894−901.

[18] ALEMDAG Y, BEDER M. Microstructural, mechanical and tribological properties of Al−7Si−(0−5)Zn alloys [J]. Mater Design, 2014, 63: 159−167.

[19] KASHYAP K T, MURALI S, RAMAN K S, MURTHY K S S. Casting and heat-treatment variables of Al−7Si−Mg alloy [J]. Mater Sci Tech, 1993, 9: 189−204.

[20] RANA R S, PUROHIT R, DAS S. Reviews on the influences of alloying elements on the microstructure and mechanical properties of aluminum alloys and aluminum alloy composites [J]. International Journal of Scientific and Research Publication, 2012, 2: 1−7.

[21] ALEMDAG Y, SAVASKAN T. Mechanical and tribological properties of Al−40Zn−Cu alloys [J]. Tribology International, 2009, 42: 176−182.

[22] ALEMDAG Y, SAVASKAN T. Effects of silicon content on the mechanical properties and lubricated wear behaviour of Al−40Zn−3Cu−(0−5)Si alloys [J]. Tribology Letters, 2008, 29: 221−227.

[23] ASM International Handbook Committee. Selection and properties of non-ferrous materials [M]. Vol. 2. Ohio: ASM International, 1989.

[24] HWANG J Y, DOTY H W, KAUFMAN M J. The effects of Mn additions on the microstructure and mechanical properties of Al−Si−Cu casting alloys [J]. Mat Sci Eng A, 2008, 488: 496−504.

[25] ZHANG G H, ZHANG J X, LI B C, CAI W. Characterization of tensile fracture in heavily alloyed Al−Si piston alloy [J]. Progress in Natural Science: Materials International, 2011, 21: 380−385.

[26] ZHANG P, LI Z, LIU B, DING W. Effect of chemical compositions on tensile behaviors of high pressure die-casting alloys Al−10Si−*y*Cu−*x*Mn−*z*Fe [J]. Mat Sci Eng A, 2016, 661: 198−210.

[27] BISWAS S K. Some mechanisms of tribofilm formation in metal/metal and ceramic/metal sliding interactions [J]. Wear, 2000, 245: 178−189.

[28] MAHATO A, PERRY T A, JAYARAM V, BISWAS S K, Pressure and thermally induced stages of wear in dry sliding of a steel ball against an aluminium−silicon alloy flat [J]. Wear, 2010, 268: 1080−1090.

[29] HUTCHINGS I. Tribology: Friction and wear of engineering materials [M]. Amsterdam: Elsevier, 1992.
[30] JASIM K M, DWARAKADASA E S. Wear in Al−Si alloys under dry sliding conditions [J]. Wear, 1987, 119: 119−130.
[31] TORABIAN H, TIWARI S N, PATHAK J P. Wear characteristics of Al−Si alloys [J]. Wear, 1994, 172: 49−58.
[32] BASAVAKUMAR K G, CHAKRABORTY M. MUKUNDA P G. Influence of melt treatments on sliding wear behavior of Al−7Si and Al−7Si−2.5Cu cast alloys [J]. J Mater Sci, 2007, 42: 7882−7893.
[33] DWIVEDI D K, THAKUR P, ARJUN T S, VAIDYA H, SINGH K. Sliding wear and friction behaviour of Al−18% Si−0.5% Mg alloy [J]. J Mater Process Tech, 2004, 152: 323−328.
[34] BIDMESHKI C, SAGHAFIAN H, ABOUEI V, SHABESTARI S G, NOGHANI M T. Effect of Mn addition on Fe-rich intermetallics morphology and dry sliding wear investigation of hypereutectic Al−17.5%Si alloys [J]. J Mater Res Technol, 2016, 5: 250−258.

Zn 含量对 Al−12Si−3Cu 合金强度和磨损性能的影响

Yasin ALEMDAG[1], Murat BEDER[2]

1. Department of Mechanical Engineering, Karadeniz Technical University, Trabzon 61100, Turkey;
2. Department of Mechanical Engineering, Gumushane University, Gumushane 29100, Turkey

摘　要：系统研究 Zn 含量对重力铸造 Al−12Si−3Cu 合金强度和磨损性能的影响。通过 OM、XRD、SEM、硬度、拉伸、压缩和 Charpy 冲击测试等手段对合金的显微组织和力学性能进行评价。干滑动磨损测试采用球−盘式摩擦磨损仪。显微镜观察结果显示，基体显微组织含有 α(Al)枝晶、针状和粗 Si 颗粒及 $CuAl_2(\theta)$相。添加 Zn 导致合金中 α-固溶体的形成和粗 Si 颗粒含量的增加。随着 Zn 含量的增加，Al−12Si−3Cu−Zn 合金的硬度、屈服强度、抗拉强度、抗压强度、断裂伸长率和冲击韧性均增加；但是，当 Zn 含量为 1.5%~2%时，合金的抗拉强度、抗压强度和伸长率均降低。此外，Al−12Si−3Cu−Zn 合金的摩擦因数和体积磨损量随 Zn 含量的增加而减小。总之，在 Al−12Si−3Cu 合金中加入 Zn 可以提高其作为摩擦材料的应用潜力。

关键词：Al−Si−Cu 合金；Zn 含量；显微组织；力学性能；磨损性能

(Edited by Wei-ping CHEN)